4D Scanning Acoustic Microscopy

Sundblad, Felix Alexander

IEEE
2022-10

Sundblad , F A , Hyvönen , J T J , Holmström , A , Salmi , A & Haeggström , E 2022 , 4D Scanning Acoustic Microscopy . in 2022 IEEE International Ultrasonics Symposium (IUS) . IEEE , pp. 1-4 , 2022 IEEE International Ultrasonics Symposium (IUS) , Venice , Italy , 10/10/2022 . https://doi.org/10.1109/IUS54386.2022.9957821

http://hdl.handle.net/10138/352777
https://doi.org/10.1109/IUS54386.2022.9957821

submittedVersion

4D Scanning Acoustic Microscope

Felix Sundblad
Electronics Research Lab.
University of Helsinki
Helsinki, Finland
felix.sundblad@helsinki.fi

Jere Hyvönen
Electronics Research Lab.
University of Helsinki
Helsinki, Finland
jere.hyvonen@helsinki.fi

Axi Holmström
Electronics Research Lab.
University of Helsinki
Helsinki, Finland
axi.holmstrom@helsinki.fi

Ari Salmi
Electronics Research Lab.
University of Helsinki
Helsinki, Finland
ari.salmi@helsinki.fi

Edward Hæggström
Electronics Research Lab.
University of Helsinki
Helsinki, Finland
edward.haeggstrom@helsinki.fi

***Abstract*— Scanning acoustic microscopy (SAM) can map mechanical surface properties and topography of materials with high spatial resolution. Coded-excitation scanning acoustic microscopy (CESAM) enables high SNR while maintaining fast imaging. The high scan speed of our CESAM allows us to study how surface mechanical properties change almost in real time. The 4D scanning capability was demonstrated with a UV-curable adhesive coating. The 4D data was constructed from three spatial dimensions and one time dimension. We set the C-scan scan rate to 30 s and measured a 400 µm x 400 µm area with 175 MHz and step size of 5 µm. With 400 MHz and step size of 1.5 µm we measured one 150 µm x 150 µm plane every 30 s.**

Keywords—scanning acoustic microscopy, coded excitation, 4D mechanical imaging

I. Introduction

Scanning acoustic microscopy (SAM) can be used to map mechanical and topographical properties of materials on micron scale. The mechanical properties can be calculated from the acoustic reflection amplitude, whereas the topography is derived from simultaneous Time-of-Flight (TOF) measurements. SAM is suited to industrial applications, e.g. for non-destructive testing of material wear [1] or coatings deformation [2]. SAM has established its importance in biological research, as neither optical microscopes nor scanning electron microscopes can detect stiffness [3] and it can thus be used in cell development studies [4] etc. Furthermore, instead of obtaining data only from the sample surface, as with scanning electron microscopes or atomic force microscopes, with SAM it is also possible to image internal mechanical properties.

Coded-excitation scanning acoustic microscopy (CESAM) enables high SNR while maintaining fast imaging. The high scan speed of our CESAM [5,6] allows us to study how mechanical properties change with time. With traditional SAMs, high-SNR images usually require long scan times. To achieve high SNR, a single image may require multiple C-scans for averaging [7, 8] or imaging at several focal distances to ensure that each pixel is imaged in focus at least once [9]. The high SNR achieved with CESAM reduces the need for averaging. The scan speed of our CESAM enables fast measurements of a series of C-scans in the same area at different times. Hence, we can obtain a 4D matrix that shows the time evolution of the imaged sample. Instead of modifying the sample between the measurements, in this study the UV-curable sample was changing in real time while it was measured.

We used two different spherically focused transducers to demonstrate the 4D capabilities of our CESAM. Two transducers with different center frequencies (Table 1) were used, as there is a trade-off between scan area size, resolution, and scan time. Thus, a small region-of-interest (ROI) could be selected iteratively for imaging with high resolution, while maintaining the same scan time.

II. Materials and Methods

A. CESAM

One way to improve SNR is to increase the excitation energy. To increase this energy, either the amplitude or signal duration need to be increased. With high frequencies, increasing the amplitude might break the thin piezo disk in the transducer. In traditional SAM, high axial resolution is achieved by using short-burst excitation for accurate TOF determination; hence, increasing signal length is suboptimal. However, CESAM uses coded excitation, allowing long signal duration and accompanying increase in SNR. With pulse compression, long signals can be used without compromising the accuracy in TOF determination [5]. With CESAM, we can perform multiple C-scans at different time steps and use fast data acquisition to evaluate mechanical properties of the sample almost in real time.

Our CESAM can be used with sonic frequencies up to 1 GHz [5]. The coded signals are generated with MATLAB (2017a, MathWorks, Massachusetts, United States) and then produced with an Arbitrary Waveform Generator (M4i.6631-x8, Spectrum Instrumentation GmbH, Grosshansdorf, Germany). The produced signal is directed through a frequency doubler and amplified. An electronic switch [10] is used to first transmit the signal to the transducer and then direct the received echo signals to an amplifier and an oscilloscope (M4i.2233-x8, Spectrum Instrumentation GmbH, Grosshansdorf, Germany). Two transducers presented in Table 1, with different center frequency, were used. The transducer was translated with Thorlabs linear stages: for Z-control, a linear stepper motor (Thorlabs MTS25-Z8) with 0.05 µm resolution and 1.6 µm repeatability, for X and Y, faster brushless DC motors with optical encoders (ThorLabs MLS203-1), were used. The XY-stage has 50 nm resolution with 250 nm repeatability at speeds up to 100 mm/s.

TABLE I. TRANSDUCERS USED IN THE STUDY AND IMPORTANT PARAMETERS

Transducer parameters	T1	T2
Model and Manufacturer	V3989 Panametrics Olympus NDT Inc.	Sa15#0515#0040, Kibero Gmbh
Bandwitdth (-6 dB)	121-277 MHz	303-443 MHz
Focal distance	2.02 mm	0.34 mm
Focal depth (-6 dB)	105 μm	29 μm
Focal width (-6 dB)	7.0 μm	2.5 μm

B. Sample

Ultraviolet-light-curable adhesive coating (Norland Optical Adhesive 68) was used to demonstrate 4D-scanning capability. UV-curable gel was chosen, as it is easy to manipulate into desired shapes and the curing speed can be controlled with the intensity of the applied UV-light. The gel was applied on a glass microscope slide, (Fisherbrand 12373118, Fisher Scientific), and was then flattened with another slide by pushing the two slides together. The top slide was subsequently removed, and the gel was cured for 5 min before being immersed in distilled water immersion. After 5 min, the sample was solid enough to not diffuse into the water, i.e. while scanning. The resulting adhesive layer was (150 ± 0.4) μm (± 1 SD) thick in the region-of-interest, *cf* Fig. 1. The layer thickness was measured by comparing TOF directly from the glass slide and sample surface.

C. Scan settings

The coded excitation used with CESAM was linear frequency-modulated (FM) chirps with Gaussian amplitude modulation (AM). The FM parameters are listed in Table 2.

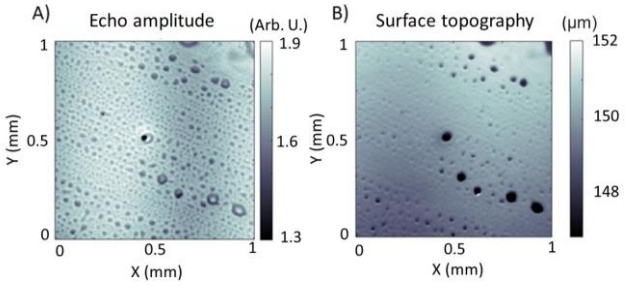

Fig. 1. A) Sample surface echo amplitude and B) height profile (TOF) measured with transducer T1. Holes left from microbubbles are visible in both amplitude and TOF maps and are aligned in the direction of top microscope slide removal. The sample is (150 ± 0.4) μm (± 1 SD) thick.

First, we selected a ROI from a larger scan (Fig. 1), re-started the curing process and imaged a series of C-scans (400 μm x 400 μm) with 175 MHz centre frequency and transducer T1 with step size of 5 μm. C-scans were taken every 30 s during a curing time of 10 min. From these series of images, we selected a smaller ROI (150 μm x 150 μm) for closer inspection with 400 MHz centre frequency and transducer T2 with step size of 1.5 μm. C-scans were taken every 30 s during a curing time of 20 min. The improved resolution achieved with T2 and higher frequency prolongs the measurement time, hence a sample-specific smaller ROI was selected. The combined measurement time was 30 minutes, Fig. 2.

III. RESULTS AND DISCUSSION

The surface of the gel layer experienced distortion in the moving water immersion, which resulted in oscillations in the recorded echo amplitude. The transducer T2 was more sensitive to the variations in surface topography than the transducer T1, due to the smaller focal depth, Table 1. For visually easier inspection of reflections from different layers, axial planes were gathered from the 4D data, *cf* Fig. 3. While measured with 400 MHz, all C-scans, two spatial and one temporal dimension, were saved as 100x100x2000 matrices, from which desired axial planes were reconstructed.

Fig. 3 reveals the sample surface and glass slide surface with 540 ns difference. Using the sample height measured in Fig 1, we estimated the speed of sound in UV-curable adhesive coating to be 560 (± 10) m/s. This applies only to the sample at the 10 min time point and with high uncertainty. Thus, we were unable to measure how the speed of sound changes as the sample was exposed to UV-light. Fig. 3 also reveals that the material is homogeneous, as we see few echoes between sample surface and glass surface.

TABLE II. CHIRP SETTINGS USED FOR CODED EXCITATION. THE FM WAS LINEAR WHILE AM HAD A GAUSSIAN ENVELOPE, WITH MAXIMUM AMPLITUDE AT THE CENTER FREQUENCY.

Transducer excitation settings	T1	T2
Centre frequency	175 MHz.	400 MHz
Start frequency	100 MHz	300 MHz
Stop frequency	250 MHz	500 MHz
Signal duration	6 μs	1 μs

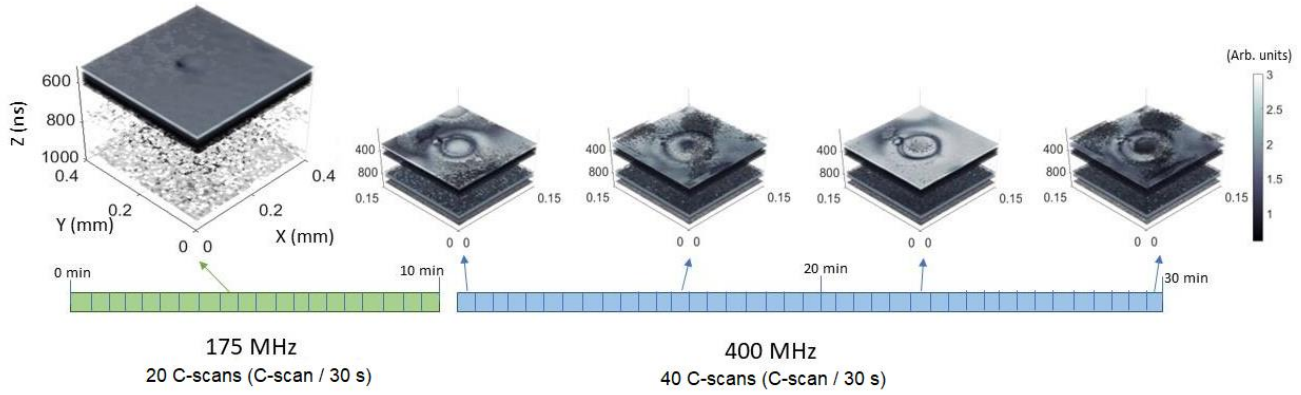

Fig. 2. C-scans were measured during 30 min with a scan rate of 30 seconds per C-scan. The curing was first inspected for 10 min with a transducer T1 (175 MHz chirp and 20 C-scans) and then with T2 (400 MHz chirp and 40 C-scans) for 20 min. In the 3D figures, the UV-gel surface and the bottom glass plate are identifiable with a time difference of 540 ns.

The suitable center frequency needed for the scan is dictated by the sample, as there is a trade-off between resolution, scan time, and scan area. With high frequencies, we achieve high resolution, but scanning the same areas requires a long time as the step size is small. Low frequencies decrease resolution, therefore, at low frequencies, the step size can be adjusted according to the transducer beam width and thus scan times are reduced. To realize this trade-off, we measured our CESAM's performance as shown in Fig. 4. Here one of the variables (scan time, step size or scan size) was kept constant, the others were changed.

Fig. 4 A) indicates that the scan speed (mm^2/s) increases with larger scans, as the relative time for acceleration and deceleration is smaller in long scan lines. Based on Fig. 4 B) exponentially more data can be collected from small scans with small step size at the same time. This indicates that less time is wasted on moving as the measuring interval is higher. For example, with a step size of 1.5 µm we obtained a 150 µm x 150 µm scan, a 100 x 100 grid in 30 s. With a 16 µm step size we can obtain a 1 mm x 1 mm scan, meaning that we only get a 63 x 63 grid, in 30 seconds. To compensate for the loss in larger scans one could scan everything in one go rather than to scan one line at a time.

Faster movement will result in more shear stress to fragile samples. The shear stress is produced by vortices induced into the immersion liquid by relative movement between the sample and the transducer. A possible solution to the problem could be protecting the sample with a thin slide and using analogue cancellation to cancel unwanted echoes from the protecting slide.

IV. Conclusions

We used our CESAM to measure changes in UV-curable resin in close to real time. The scan time depends on the scan size and the step size and should hence be selected separately for each sample depending on the required image resolution and rate of change in the sample. The acoustic reflection amplitude depended on the curing state, but also on surface roughness, as the UV-curable gel showed micrometre-sized roughness. The height variance had a bigger impact on the 400 MHz transducer, as it has smaller focal depth than the 175MHz transducer.

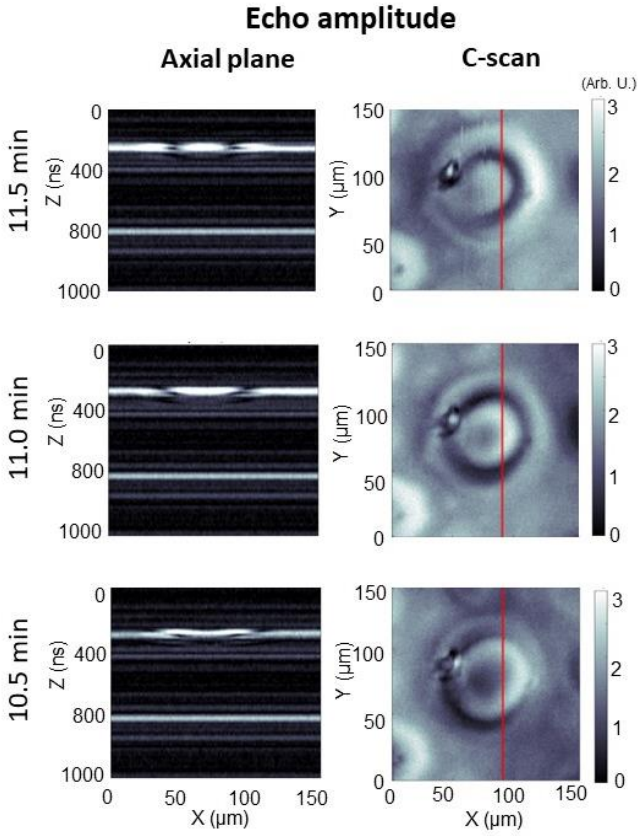

Fig. 3. Three C-scans measured with the 400 MHz transducer over 1.5 minutes. Desired axial planes were selected from C-scans (red line) to inspect the curing inside the sample. From the axial planes, it was possible to identify the gel surface (at 290 ns) and glass surface (at 830 ns). The change in the bubble formation was evident in the axial plane.

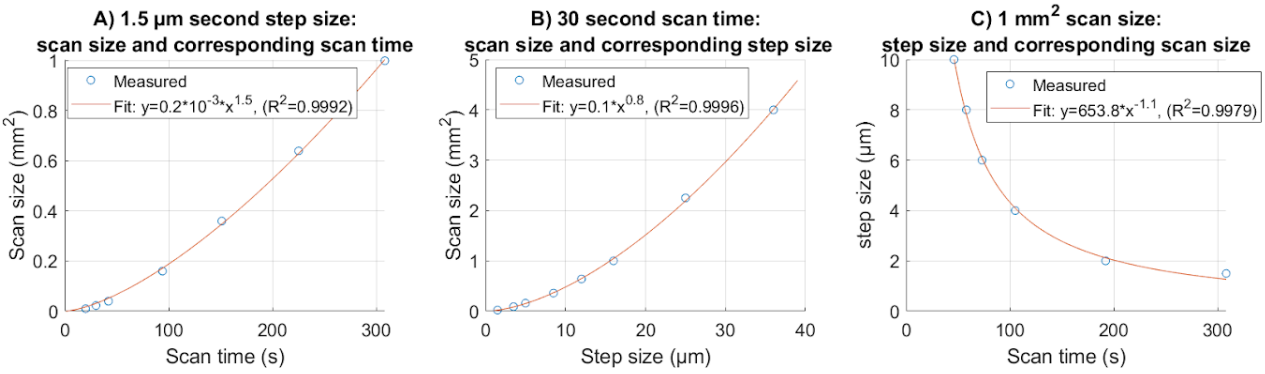

Fig. 4 A) We performed multiple scans of different sizes with step size of 1.5 µm and measured scanning time. B) Comparison between scan size and step size while the scan time is limited to 30 seconds. C) Step size as a function of scanning time, while the measured area was constant (1 mm^2). Based on the figures, the trade-off is not linear between the scan time, step size and scan size.

REFERENCES

[1] K. Yamanaka, Y. Enomoto, and Y. Tsuya, “Application of Scanning Acoustic Microscope to the Study of Fracture and Wear,” Acoustical Imaging, vol 12. Springer, Boston, 1982.

[2] B. Reddy and J.M. Sykes, “Degradation of organic coatings in a corrosive environment: a study by scanning Kelvin probe and scanning acoustic microscope,” Prog. in Org. Coat., vol. 52, Issue 4, 2005, pp. 280-287.

[3] R. A. Lemons and C. F. Quate, “Acoustic microscopy: Biomedical applications,” Science, vol. 188, no. 4191, pp. 905–911, 1975.

[4] E. M. Strohm, G. J. Czarnota and M. C. Kolios, "Quantitative measurements of apoptotic cell properties using acoustic microscopy," in IEEE Trans Ultrason Ferroelectr Freq Control, vol. 57, no. 10, pp. 2293-2304, October 2010.

[5] Antti Meriläinen, Jere Hyvönen, Ari Salmi, and Edward Hæggström, ”CESAM-coded exitation scanning acoustic microscope”, Rev. Sci. Instrum, vol. 92, no. 74901, 2021.

[6] J. Hyvönen, A. Meriläinen, A. Salmi, L. Hupa, N. Lindfors and E. Hæggström, "Three Megapixel Ultrasonic Microscope Imaging," IEEE Int Ultrason. Symp., pp. 1886-1889, 2019.

[7] E. C. Weiss, P. Anastasiadis, G. Pilarczyk, R. M. Lemor and P. V. Zinin, "Mechanical Properties of Single Cells by High-Frequency Time-Resolved Acoustic Microscopy," in IEEE Trans Ultrason Ferroelectr Freq Control, vol. 54, no. 11, pp. 2257-2271, Nov. 2007.

[8] O. Balogun, G. D. Cole, R. Huber, D. Chinn, T. W. Murray and J. B. Spicer, "High-spatial-resolution sub-surface imaging using a laser-based acoustic microscopy technique," in IEEE Trans Ultrason Ferroelectr Freq Control, vol. 58, no. 1, pp. 226-233, January 2011.

[9] K. Raum, K. V. Jenderka, A. Klemenz and J. Brandt, "Multilayer analysis: quantitative scanning acoustic microscopy for tissue characterization at a microscopic scale," in IEEE Trans Ultrason Ferroelectr Freq Control, vol. 50, no. 5, pp. 507-516, May 2003.

[10] A. Meriläinen, T. Fabritius, J. Eskelinen and E. Hæggström, “Solid state switch for gigahertz coded signal ultrasound microscopy,” in Electron. Lett., vol. 49, pp. 169-170, 2013.